Hybridization of Silicon/Carbon Composites with Natural Graphite for Improving Anodic Performances of Lithium-Ion Batteries

Park, Tae-Hwan
Interdisciplinary Graduate School of Engineering Sciences, Kyushu University

Yeo, Jae-Seong
Institute for Materials Chemistry and Engineering, Kyushu University | Interdisciplinary Graduate School of Engineering Sciences, Kyushu University

Seo, Min-Hyun
Institute for Materials Chemistry and Engineering, Kyushu University

Miyawaki, Jin
Institute for Materials Chemistry and Engineering, Kyushu University

他

出版情報：Journal of Novel Carbon Resource Sciences. 6, pp.24-28, 2012-09. Kyushu University G-COE program "Novel Carbon Resource Sciences" secretariat
バージョン：
権利関係：

Kyushu University Global COE Program
Journal of Novel Carbon Resource Sciences, Vol. 6, pp. 24-28, Sep. 2012

Hybridization of Silicon/Carbon Composites with Natural Graphite for Improving Anodic Performances of Lithium-Ion Batteries

Tae-Hwan Park[*1], Jae-Seong Yeo[*1], Min-Hyun Seo[*2], Jin Miyawaki[*2], Isao Mochida[*3], Seong-Ho Yoon[*2]

[*1]Interdisciplinary Graduate School of Engineering Sciences, Kyushu University
[*2]Institute for Materials Chemistry and Engineering, Kyushu University
[*3]Research and Education Center of Carbon Resources, Kyushu University

(Received June 7, 2012; accepted July 4, 2012)

Hybrid composites of silicon/pyrolytic carbon/carbon nanofiber (Si/PyC/CNF) with natural graphite were synthesized as a means of improving the anodic performance of Li-ion batteries. Samples made with hybridization levels of 10–30 wt% exhibited excellent cyclability with a discharge capacity of over 400 mAh/g. Si/PyC/CNF composites showed better hybridization effects on cyclability than composites containing Si/PyC. These effects were attributable to the more homogeneous dispersion of Si/PyC/CNF in the electrode material. The internal spaces created under such circumstances may prevent electrode destruction by relieving tensions induced by the expansion of Si particles in the electrode over the course of repeated charge and discharge processes.

1. Introduction

Recently, research into large-scale, Li-ion batteries has been ramped up for applications in electric vehicles and as large-scale backup power supplies. Such applications require carbon anode materials with high rate capabilities and long lifetimes. Natural graphite is still considered an important anodic material in Li-ion batteries due to its high reversible capacity, flat voltage profile, good cyclability, and low cost. However, the discharge capacity, rate capability, and cyclability of natural graphite are not still sufficient for high-power density batteries[1–3].

Among many candidate anodic materials boasting high capacity, silicon-based materials such as Si, SiO, and Si–metal alloys have attracted considerable interest. However, extensive volumetric changes with charging and discharging result in a rapid decrease in capacity. Many efforts have attempted to overcome this problem, including reducing the particle size[4, 5] and using Si-based thin films and nanowires[6, 7], and composite materials[8–10]. Among these strategies, the most promising is the combination of nano-sized silicon with carbon materials[11–15]. In these materials, the carbon component acts as both a structural buffer and an agent for enhancing electric conductivity.

In a previous study, we described a Si/carbon nanofiber (CNF) composite with improved cyclability and a high discharge capacity. These enhancements were due to CNF on the surface of the silicon particles, which suppressed volume expansion by providing adequate space in the electrode[11]. The present study examined the hybridization effects of two Si/carbon composites (nano-sized Si/pyrolytic carbon-coated composite (Si/PyC) and nano-sized Si/pyrolytic carbon-coated/CNF composite (Si/PyC/CNF)) with natural graphite (NG) on the discharge capacity and cyclability of Li-ion batteries. Two different sizes of silicon nanoparticles were evaluated to determine the effects of particle size on the pyrocarbon coating and CNF composite.

2. Experimental

2.1 Sample preparation

Nano-sized silicon particles with average diameters of 20 nm and 50 nm (Nanostructured & Amorphous Materials, Inc., Houston, TX) and natural graphite (5 μm averaged diameter, MAG; Hitachi Kasei, Tokyo, Japan) were used as starting materials. High-purity helium, methane, carbon monoxide, and hydrogen gases were used for pyrolytic carbon (PyC) coating and CNF growth.

PyC coating of the Si particles was carried out in a general horizontal furnace using a quartz boat. Si particles in the boat were heated to 900 °C at a heating rate of 10 °C min^{-1} under He flow. When the temperature reached 900 °C, the gas flow was changed to a mixture of CH_4 and Ar (4:1) and kept for 1 h. The amounts of PyC were controlled at 21 wt% for 20-nm Si particles and 19 wt% for 50-nm Si particles. The obtained PyC-coated Si particles were designated as Si/PyC. Iron nitrate nonahydrate [$Fe(NO_3)_3 \cdot 9H_2O$] (reagent grade; Wako Pure Chemical Industries Ltd., Osaka, Japan) was dissolved in ethanol and the solution was stirred for 3 h at room temperature to disperse the Fe catalyst over the Si/PyC particles. The amounts of catalyst were carefully controlled at 2 wt% Fe based on the Si/PyC weight. After evaporating the ethanol at 55 °C, the mixture was dried at 50 °C for 24 h under vacuum. CNF was grown on the surface of the Si/PyC particles in a fixed-bed reactor. The Si/PyC particles with 2 wt% Fe catalyst were placed in the center of a horizontal tube furnace and heated to 600 °C at a rate of 10 °C min^{-1} under He flow. Then a mixed gas of CO and H_2 was introduced for 30 min. The amounts

of CNF were estimated at 32 wt% for the 20-nm Si/PyC particles and 75 wt% for the 50-nm Si/PyC particles. The obtained particles were designated as Si/PyC/CNF.

2.2 Analysis and electrochemical tests

The morphologies of Si, Si/PyC, and Si/PyC/CNF particles were observed using a transmission electron microscope (TEM, JEM-2100F; JEOL, Tokyo, Japan). Crystallographic properties were measured with an X-ray diffractometer (XRD, CuKα, Ultima-III; Rigaku, Tokyo, Japan). Galvanostatic charge/discharge experiments were carried out using a coin-type CR2032 cell with two electrodes. Li metal foil was used as the counter electrode. Styrene–butadiene rubber (SBR, trade name BM-400B; ZEON, Tokyo, Japan), which has a high tensile strength and greater flexibility and higher thermal stability than poly(vinylidene fluoride) (PVDF)[16], was used with carboxymethyl cellulose (CMC) as a binder system (anode material : SBR : CMC = 90 : 7 : 3 wt%). The mixed slurry was coated onto copper foil (18 μm thick) or nickel foam as current collectors. The electrodes were then dried at 120 °C under vacuum for 12 h before pressing into a roll-type mill under 100 MPa of pressing pressure. The pressed electrode was cut into discs (12 mm diameter and 60 μm thick) and weighed with an ultra-fine balance to control the amount of active material. Coin-type cells were assembled in Ar-filled glove box using a polyethylene film (16 μm thick) as a separator and 1 M $LiPF_6$ in ethylene carbonate (EC)/diethyl carbonate (DEC) (1 : 1 vol%; Ube Kosan, Tokyo, Japan) as an electrolyte. The electrochemical measurements were performed through charging at constant current–constant voltage (CCCV) and discharging at constant current (CC) with a current density of 30 or 100 mA/g over the potential range of 0.003–1.5 V versus Li/Li^+ (Toscat-3100; Toyo System, Tokyo, Japan) at room temperature. Electrochemical impedance spectroscopic (EIS) studies were performed by applying a small perturbation voltage of 5 mV over the frequency range of 100 kHz to 160 mHz at 0.9 V.

3. Results and discussion

3.1 Analytical results of Si/PyC and Si/PyC/CNF

Fig. 1 shows diffractograms of Si, Si/PyCs, and Si/PyC/CNF nanoparticles. After pyrolytic carbon coating of the Si particles, a small amorphous carbon peak corresponding to C (002) was observed at approximately 25°. The Si/PyC/CNF particles yielded a large peak due to the CNF.

Fig. 2 shows TEM images of Si/PyC and Si/PyC/CNF particles. Very thin layers of pyrolytic carbon less than 4 nm thick were observed coating the surfaces of both the 20-nm (20Si) and 50-nm (50Si) silicon particles (Fig. 2(a) and (c)). Also, the grown CNF particles, with diameters of approximately 10 nm, were observed on the surface of the Si/PyC/CNFs (Fig. 2(b) and (d)).

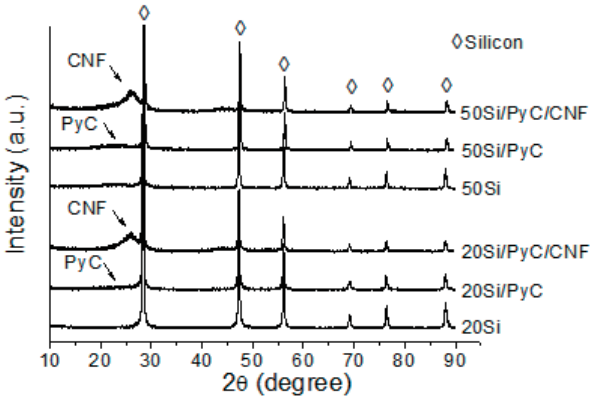

Fig. 1 XRD profiles of Si particles and Si-carbon composites.

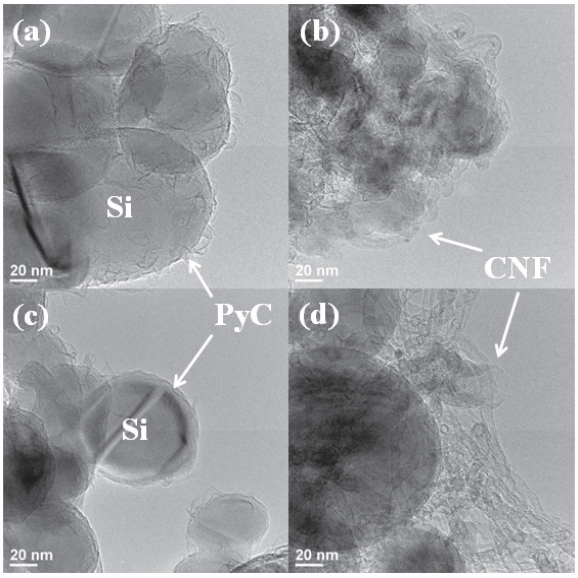

Fig. 2 TEM images of (a) 20Si/PyC, (b) 20Si/PyC/CNF, (c) 50Si/PyC, and (d) 50Si/PyC/CNF.

3.2 Electrochemical properties of Si particles and Si/carbon composites

Fig. 3 shows the cyclability of Si particles and Si/carbon composites at a current density of 100 mA/g. Both the Si particles and the Si/PyC composites exhibited lower cyclability than the Si/PyC/CNF composites. The cyclability of the 50Si/PyC/CNF composite was more stable than that of the 20Si/PyC/CNF (32 wt% Si), which can be ascribed to the higher CNF composition of the former (75 wt% Si). The 50Si/PyC/CNF composite had a discharge capacity of 960 mAh/g with 95% capacity retention after 30 charge/discharge cycles.

Fig. 4 shows typical Nyquist plots of the Si, Si/PyC, and Si/PyC/CNF materials discharged to 0.9 V. The measured impedance data over the entire frequency range can be analyzed using an equivalent circuit[17]. The film and charge transfer resistances increased in the order of Si > Si/CNF > Si/PyC/CNF. The excellent cyclability of the Si/PyC/CNF composite may be due to its inherently lower resistance.

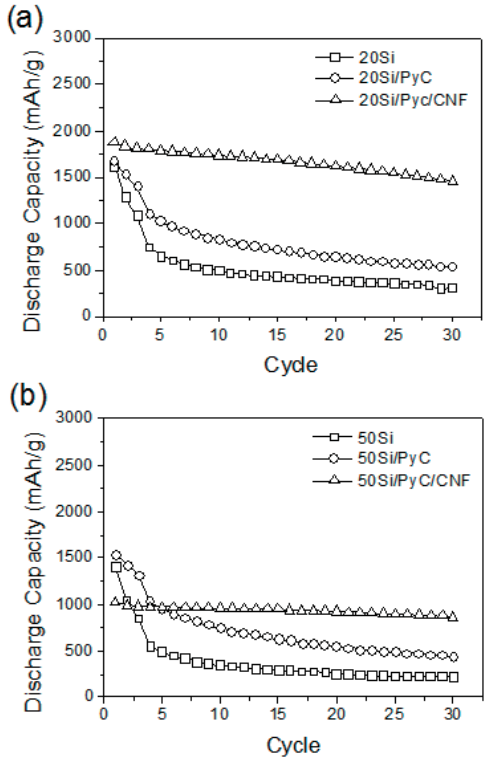

Fig. 3 Cycle-abilities of the Si particles and Si-carbon composites at the current density of 100 mA/g (a) 20Si, 20Si/PyC, and 20Si/PyC/CNF, (b) 50Si, 50Si/PyC, and 50Si/PyC/CNF.

3.3 Hybridization effects on the cyclability of Si-carbon composites with natural graphite

Fig. 5 shows the cyclabilities of Si/PyC-mixed natural graphite hybridized materials at a current density of 30 mA/g. In Fig. 5(a), the sample containing 10 wt% 20Si/PyC-mixed natural graphite (20Si/PyC : NG = 1 : 9) showed relatively high cyclability with a large discharge capacity of over 500 mAh/g while maintaining a capacity retention of 94.8% after 30 cycles. The 1st cycle Coulombic efficiency was as high as 89.8%. However, the 20 and 30 wt% composites (20Si/PyC : NG = 2 : 8 and 20Si/PyC : NG = 3 : 7) exhibited significant decays in capacity after 15 cycles with retentions of only 84.7% and 79.9%, respectively, after 30 cycles.

Fig. 5(b) shows that the 10 wt% 50Si/PyC-mixed sample (50Si/PyC : NG = 1 : 9) also exhibited relatively high cyclability with an improved discharge capacity of over 450 mAh/g while retaining 100% of its capacity over 30 cycles. The 1st cycle Coulombic efficiency was as high as 89.2%. However, the 2 : 8 50Si/PyC : NG sample showed a significant capacity decay after 15 cycles and resulted in a capacity retention of 88.8% after 30 cycles. The capacity of the 30 wt% sample (50Si/PyC : NG = 3 : 7) decayed even before the 10th cycle and exhibited a capacity retention of 81.8%. The observed dependence of cyclability on Si particle size suggests that larger Si particles experience more severe deterioration (i.e., surface cracking) during lithium-ion insertion and extraction processes.

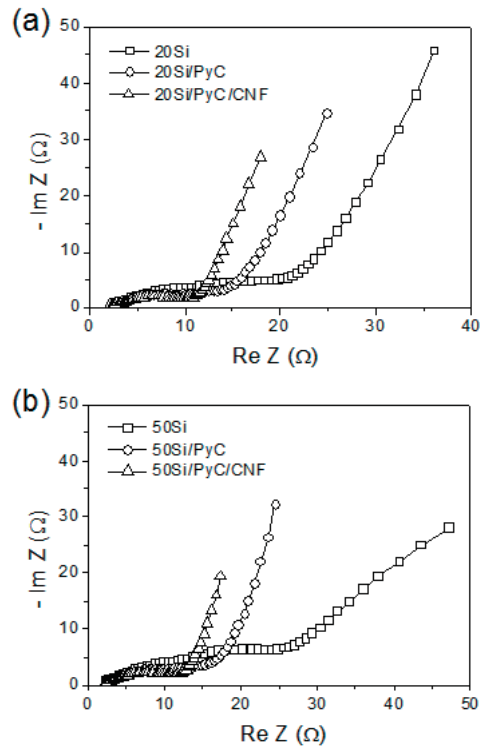

Fig. 4 Typical Nyquist plots of the Si particles and Si-carbon composites discharged to 0.9 V (a) 20Si, 20Si/PyC, and 20Si/PyC/CNF, (b) 50Si, 50Si/PyC, and 50Si/PyC/CNF.

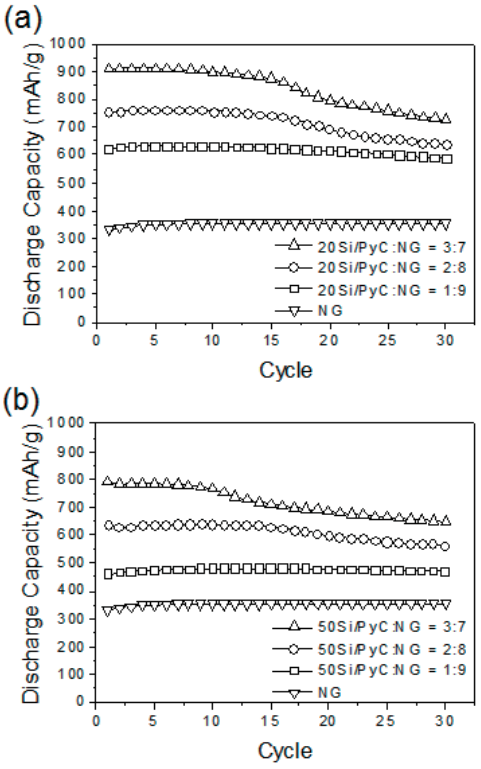

Fig. 5 Cycle-ability of Si/PyC mixed natural graphite hybridized materials at the current density of 30 mA/g, (a) 20Si/PyC mixed natural graphite hybridized materials, (b) 50Si/PyC mixed natural graphite hybridized materials.

Fig. 6 shows the cyclability of Si/PyC/CNF-mixed natural graphite hybridized materials at a current density of 30 mA/g. Fig. 6(a) shows that the 1 : 9 20Si/PyC/CNF : NG sample exhibited high cyclability with a discharge capacity of 450 mAh/g while maintaining 97.7% of its initial capacity after 30 cycles. It also showed a relatively high 1st cycle Coulombic efficiency of 80.3%. In contrast with the Si/PyC-mixed natural graphite hybridized materials, the 2 : 8 20Si/PyC/CNF : NG and the 3 : 7 20Si/PyC/CNF : NG did not suffer from a sudden decay in cyclability until after 30 charge/discharge cycles. These composites also exhibited discharge capacities of over 550 mAh/g and over 650 mAh/g, respectively, while maintaining capacity retention ratios of 94.5% and 92.6% after 30 cycles. The 1st cycle Coulombic efficiencies were also improved to 74.2% and 67.5%, respectively, relative to that of the 20Si/PyC/CNF composite.

Fig. 6(b) shows excellent cyclability for the 1 : 9 50Si/PyC/CNF : NG composite with a discharge capacity of 420 mAh/g while maintaining a capacity retention of 98.8% after 30 cycles. It also yielded a relatively high 1st cycle Coulombic efficiency of 77.8%. The 2 : 8 50Si/PyC/CNF : NG and 3 : 7 50Si/PyC/CNF : NG composites also showed stable cyclabilities until after 30 cycles. These composites had discharge capacities of over 495 mAh/g and over 520 mAh/g while maintaining capacity retentions of 96.7% and 95.4% after 30 cycles, respectively. The 1st cycle Coulombic efficiencies were 72.1% and 66.9%, respectively, relative to that of the 50Si/PyC/CNF composite.

The Si/PyC/CNF-mixed natural graphite hybridized materials exhibited higher cyclability than the Si/PyC-mixed natural graphite hybridized samples. Therefore, the CNF effectively stabilized cyclability through suppression of electrode expansion during charge and discharge cycles. Homogeneous dispersion of Si/PyC/CNF may have created internal spaces within the electrode, which would prevent electrode deterioration by relieving the tension induced by the expansion of Si particles in the electrode[11]. Fig. 7 shows a schematic of the volumetric changes occurring in electrodes composed of the Si/PyC-mixed natural graphite and Si/PyC/CNF-mixed natural graphite hybridized materials.

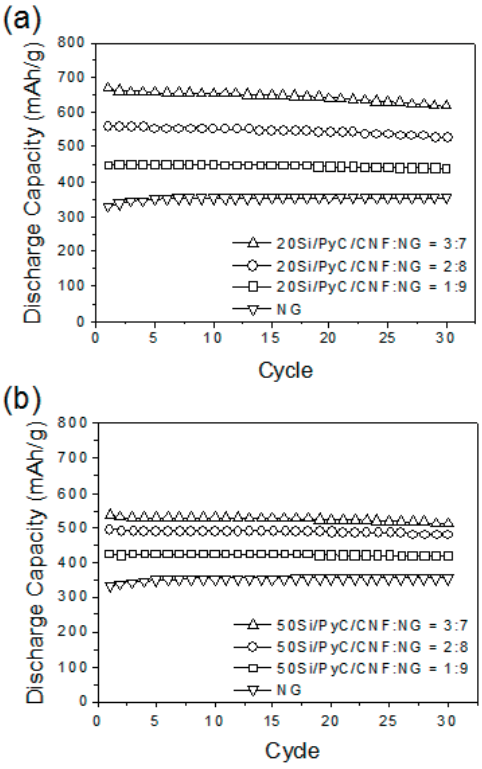

Fig. 6 Cycle-ability of Si/PyC/CNF mixed natural graphite hybridized materials at the current density of 30 mA/g, (a) 20Si/PyC/CNF mixed natural graphite hybridized materials, (b) 50Si/PyC/CNF mixed natural graphite hybridized materials.

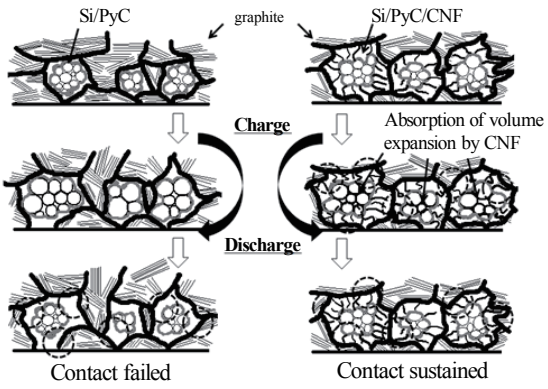

Fig. 7 Schematic models of the morphological changes of Si/PyC and Si/PyC/CNF mixed natural graphite electrodes during the charge and discharge processes.

4. Conclusions

The effects of hybridization on the cyclability of a Li-ion battery system were evaluated for two kinds of Si/carbon composites with natural graphite. The effects of Si particle size were also examined by using Si nanoparticles with different diameters. The data suggest the following:

(1) Cyclability increased in the order of Si/PyC/CNF > Si/PyC > Si. The Si/PyC/CNF composites had lower intrinsic resistance than the Si/PyC or Si materials.

(2) The cyclability of Si/PyC/CNF-mixed natural graphite hybridized materials was more stable than that of the Si/PyC-mixed natural graphite hybridized composites.

(3) The 20Si/PyC-mixed natural graphite composites exhibited higher cyclability than the 50Si/PyC-mixed natural graphite composites. These data suggest that smaller Si particles allow more stable cyclability.

(4) The addition of CNF to the Si/PyC composites stabilized cyclability through the suppression of electrode expansion during charge and discharge processes.

(5) The hybridization of Si/PyC/CNF with natural graphite could support the deficient discharge capacity of natural graphite for usage of electric vehicles.

References

1) A. Naji, P. Willmann, D. Billaud, *Carbon*, **36**, 1347 (1998).
2) Y. Yamauchi, T. Hino, K. Ohzeki, Y. Kubota, S. Deyama, *Carbon*, **43**, 1334 (2005).
3) S. Yoon, C. Park, H. Yang, Y. Korai, I. Mochida, R. Baker, *Carbon*, **42**, 21 (2004).
4) J. Graetz, C. Ahn, R. Yazami, B. Fultz, *Solid-State Lett.*, **6**, A194 (2003).
5) H. Kim, M. Seo, M. Park, J. Cho, *Angew. Chem. Int. Ed.*, **49**, 2146 (2010).
6) K. Lee, J. Jung, S. Lee, H. Moon, J. Park, *J. Power Sources*, **129**, 270 (2004).
7) C. Chan, H. Peng, G. Liu, K. Mcllwrath, X. Zhang, R. Huggins, Y. Cui, *Nature Nanotech.*, **3**, 31 (2008).
8) Y. Liu, K. Hanai, J. Yang, N. Imanishi, A. Hirano, Y. Takeda, *Solid State Ionics*, **16**, 861 (2004).
9) M. Yoshio, T. Tsumura, N. Dimov, *J. Power Sources*, **163**, 215 (2006).
10) Y. Hu, R. Demir-Caken, M. Titirici, J. Muller, R. Schlogl, M. Antonitti, J. Maier, *Angew. Chem. Int. Ed.*, **47**, 1645 (2008).
11) S. Jang, J. Miyawaki, M. Tsuji, I. Mochida, S. Yoon, *Carbon*, **47**, 3383 (2009).
12) H. Habazaki, M. Kiriu, H. Konno, *Electrochem. Commun.*, **8**, 1275 (2006).
13) Q. Si, T. Hanai, T. Hirano, N. Imanishi, Y. Takeda, O. Yamamoto, *J. Power Sources*, **195**, 1720 (2010).
14) F. Cheng, Z. Tao, J. Liang, *J. Chen, Chem. Mater.*, **20**, 667 (2008).
15) L. Ji, X. Zhang, *Electrochem. Commun.*, **11**, 1146 (2009).
16) M. Yoshio, S. Kugino, N. Dimov, *J. Power Sources*, **153**, 375 (2006).
17) M. Levi, D. Aurbach, *J. Phys. Chem.*, **B101**, 4630 (1997).